A single grain approach applied to modelling recrystallization kinetics in a single-phase metal

Document Version:
Publisher's PDF, also known as Version of Record (includes final page, issue and volume numbers)

Please check the document version of this publication:

• A submitted manuscript is the version of the article upon submission and before peer-review. There can be important differences between the submitted version and the official published version of record. People interested in the research are advised to contact the author for the final version of the publication, or visit the DOI to the publisher's website.
• The final author version and the galley proof are versions of the publication after peer review.
• The final published version features the final layout of the paper including the volume, issue and page numbers.

Link to publication

Download date: 04. Oct. 2023

A Single-Grain Approach Applied to the Modeling of Recrystallization Kinetics for Cold-Rolled Single-Phase Metals

S.P. CHEN and S. VAN DER ZWAAG

A comprehensive model for the recrystallization kinetics is proposed which incorporates both microstructure and the textural components in the deformed state. The model is based on the single-grain approach proposed previously. The influence of the as-deformed grain orientation, which affects the stored energy *via* subgrain size and sub-boundary misorientation, is taken into account. The effects of the deformed grain geometry, the nucleation-site density, and the initial grain size prior to deformation on the recrystallization kinetics are assessed. The model is applied to the recrystallization kinetics of a cold-rolled AA1050 alloy.

I. INTRODUCTION

THE recrystallization kinetics in simple metallic systems is frequently described by JMAK-type models.[1] The basis of the JMAK analysis, which yields the volume fraction transformed (X) against time (t), is

$$X = 1 - \exp(-kt^n) \qquad [1]$$

The constant k involves the nucleation rate, or the nucleation-site density, and the growth rate. The exponent n relates to the time dependencies of the nucleation rate, growth, and dimensionality of the growth fronts. The crucial assumption made in deriving the various forms of JMAK is that the nucleation sites are randomly distributed in space, leading to n values of 3 or 4. However, in almost all experimental studies of recrystallization kinetics in aluminum alloys, the exponent n is less than 2. Such a deviation from ideal JMAK behavior is attributed to be the occurrence of concurrent recovery,[2] or a nonuniform distribution of stored energy.[3,4]

The occurrence of the simultaneous recovery during recrystallization will reduce the dislocation density and, hence, the stored energy. Consequently, the concurrent recovery should retard recrystallization kinetics and cause a negative deviation from linear JMAK behavior. However, both experiments[5,6] and theoretical predictions[3,7] have shown that concurrent recovery cannot fully explain the observed lower value for n. Hence, a more detailed analysis of the uniformity of stored energy in deformed metals and its effect on the recrystallization behavior seems appropriate.

It is well known that the deformation in a polycrystal material is inhomogeneous.[8,9] The inhomogenity is of a dual nature. First, the area along the original grain boundaries undergoes a more severe plastic deformation than that along the average macroscopic level. As a result, a deformation gradient will form in the grain; the original grain boundaries are of highest dislocation density and, therefore, are the main source of recrystallization nuclei, especially for single-phase alloys. Like the effect of concurrent recovery, this kind of inhomogenity also leads to a time-dependent growth rate of recrystallizing grains and, therefore, reduces the slope of the JMAK plot. However, it was found that continuous reductions in growth rate by a factor of 10 were required to cause the JMAK exponent to drop significantly below a value of 3. The variation in growth rate by a factor of 2 in real experiment caused no detectable change in the simulated exponent.[10,11] Furthermore, this explanation cannot be applied to cases where the nucleation is on a coarser scale than the distribution of the stored energy.

The second inhomogenity refers to the fact that the deformation microstructure varies from grain to grain because of the initial crystallographic texture. As a result, the nucleation sites for recrystallization in deformed grains with different orientations are different.[12,13] Each as-deformed grain will recrystallize at a rate that depends on its size as well as initial orientation with respect to the deformation field, depending on the accumulation of the stored energy. Hence, the nonuniformity of the recrystallization behavior is most likely due to the variation of the stored energy as a function of the grain orientation. Dillamore and Katoh[14] have pointed out that the variation of stored energy as a function of the texture is related to the variation of the Taylor factor. The order of the amount of the stored energy of the deformation textures in low-carbon steel is[15] $E_{\{110\}<110>} > E_{\{111\}<uvw>} > E_{\{211\}<011>} > E_{\{100\}<011>}$. The dislocation structures and density in aluminum alloys were observed to be dependent on the crystallographic orientation too, although there was a wide scatter in the experimental data.[16,17]

In addition, it has been realized that the recrystallization kinetics and the resulting grain structures are determined by the ratio of the nucleation to the growth rate, the density and spatial distribution of nucleation sites, as well as the impingement space. All these factors are strongly dependent on the microstructure, the substructures in individual grains, and the local orientations between grains, developed during plastic deformation. Therefore, a more realistic recrystallization model should take into account all these details of a deformed microstructure.

The advanced techniques such as electron backscattered diffraction and hard X-rays from a synchrotron source make it possible to examine the recrystallization behaviors at the level of an individual grain.[8,18,19] However, theoretical models at this level are still lacking. In Reference 7, we have proposed

S.P. CHEN, Postdoctor, formerly with NIMR (Netherlands Institute for Metal Research), Delft University of Technology, is now with NIMR, Faculty of Mechanical Engineering, Eindhoven University of Technology, Eindhoven, The Netherlands. S. VAN DER ZWAAG, Professor, is with the Faculty of Aerospace Engineering, Delft University of Technology, 2629HS Delft, The Netherlands. Contact e-mail: s.vanderzwang@lr.tudelft.nl
Manuscript submitted June 14, 2002.

a single-grain approach to predict the recrystallization kinetics of a polycrystal aggregate. The structure of the deformed metal is taken into account in the model, which contains the information about the main features of rolled material, *i.e.*, on the degree of cold rolling, the grain size, and the grain shape. An as-deformed tetrakaidecahedron is applied to describe the grain geometry. The grain-shape change with strain is introduced through a parameter of aspect ratio according to the macroscopic change in the shape of the specimen (principle of the Taylor model). Additionally, the subgrain size and the misorientation between subgrains belonging to the same grain are related to the degree of deformation.

In the present article, the physical model of the recrystallization kinetics, based on the single-grain approach, is further developed to incorporate both microstructural inhomogeneities and the textural components in the as-deformed state. The influence of the as-deformed grain orientation, which affects the stored energy *via* subgrain size and sub-boundary misorientation, is taken into account. The effect of the initial grain size, the grain geometry, and the nucleation-site density on the recrystallization kinetics is assessed. The model is applied to the recrystallization kinetics in cold-rolled AA1050.

II. EXPERIMENTS

The AA1050 studied has a chemical composition of 0.185 wt pct Fe, 0.109 wt pct Si, and the balance Al. A cold-rolled plate with a thickness of 5 mm was annealed at 600 °C for 2 hours and quenched in water. The material was then subjected to a precipitation treatment at 400 °C for 2 hours to reduce and stabilize the content of iron in solid solution. The average grain size after this treatment was 98 ± 5 μm. Metallographic examination revealed a coarse (2 to 4 μm) iron-rich constituent produced during casting and fine (0.1 to 0.3 μm) precipitates resulting from annealing. Following a cold-rolling treatment leading to a reduction of 50 pct in thickness ($\varepsilon = 0.69$), the samples were annealed in a salt bath at 340 °C for a range of times and then quenched in water to get different degrees of recrystallization. All the metallographical and orientation imaging microscopy (OIM) observations were confined to the center layer of the sample. The OIM facility performed a scan over an area of 1200×600 μm^2, containing approximately 120 deformed grains. The degree of recrystallization was determined quantitatively and accurately using the method described in Reference 20.

Five typical orientations of grains in the deformed state, namely, cube {100}<001>, Goss {110}<100>, brass {110}<112>, S {124}<211>, and copper {112}<110>,

are observed in OIM analysis. The frequency of the texture components in the as-deformed state is listed in Table I. The average fully recrystallized grain size after deformation to a strain of 0.69 and annealing at 340 °C was 69 ± 5 μm.

Figure 1 shows a partially recrystallized structure in a sample annealed at 340 °C for 50 minutes, showing the characteristic of the inhomogeneous nucleation. Recrystallization was found to occur faster in the grains with copper and/or S orientations. Grains with a cube orientation are the slowest to recrystallize.

The overall recrystallization kinetics as measured by optical microscopy is shown in Figure 2 by the square dotted line. Also in this figure, we illustrate schematically the approximate recrystallization kinetics examined in grains with different orientations by OIM.

III. MODELING THE RECRYSTALLIZATION KINETICS

A. *The Orientation-Dependent Microstructure in the Deformed State*

The dislocation density within a given grain after plastic deformation is primarily related to the amount of crystallographic slip (Γ), which is defined as[21]

$$\Gamma = M\varepsilon \qquad [2]$$

where M is the orientation factor of the as-deformed grain (Taylor factor), and ε is the macroscopic shape change (true strain) of the grain, which is assumed to be the same as that of the specimen.

As an approximation, we assume that aluminum follows a linear strain-hardening behavior, *i.e.*,

$$\tau_c - \tau_0 = \beta\Gamma \qquad [3]$$

where τ_c is the resolved shear stress, τ_0 is the frictional part of τ_c, and β is a constant.

The relationship between the internal stress and dislocation density can be written as

$$\tau_c - \tau_0 = \beta' \sqrt{\rho} \qquad [4]$$

where β' is another constant. Combining Eqs. [3] and [4], one obtains

$$\rho \propto \Gamma^2 \qquad [5]$$

In most cases, and certainly for this aluminum grade, the dislocations are arranged in a cellular substructure or into a

Table I. The Taylor Factor of the Main Texture Components and Related Substructural Parameter Values after Cold Rolling 50 percent

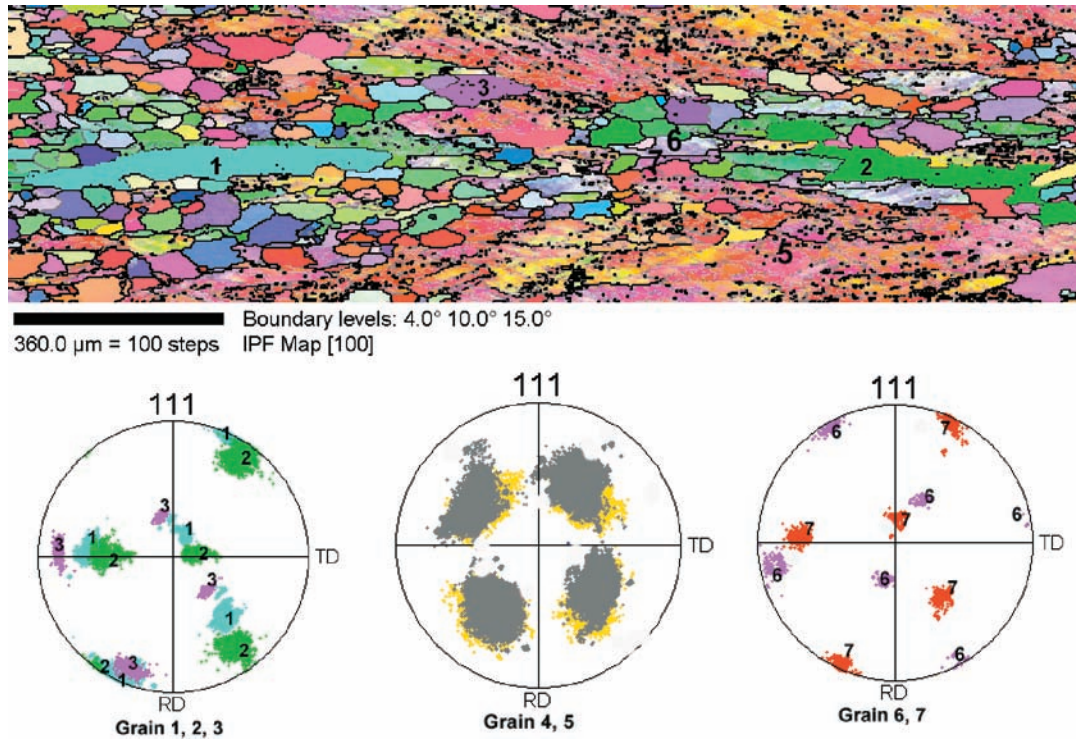| Texture Component	{*hkl*}<*uvw*>	*M* Value	δ (μm)	θ	Frequency (Pct)
RG	{011}<110>	4.90	0.46	4.68	0
Copper	{112}<111>	3.67	0.61	3.53	2
S	{123}<364>	3.52	0.64	3.34	7
Brass	{011}<211>	3.27	0.68	3.15	9
Goss	{011}<100>	2.75	0.82	2.63	20
Cube	{001}<100>	2.45	0.94	2.29	13
Random		3.06	0.73	2.92	49
		average			

Fig. 1—OIM of an AA1050 sample annealed at 340 °C for 50 min, showing the inhomogeneous nature of the recrystallization process.
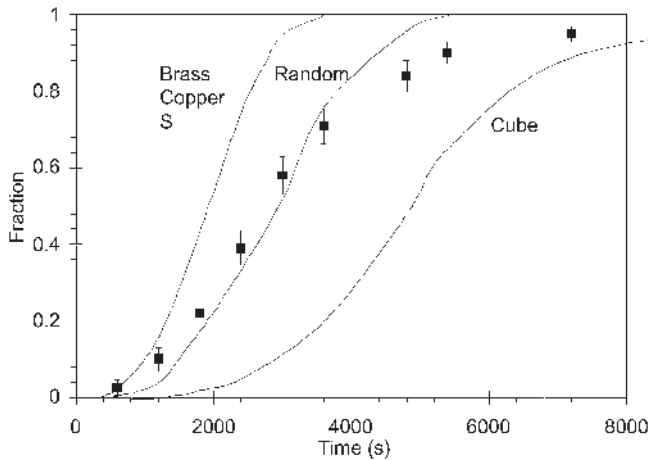

Fig. 2—The overall softening kinetics measured by optical microscopy (square marks) and approximate recrystallization kinetics of three texture components at 340 °C after a strain of 0.69.

subgrain. If the substructure in a specific deformed grain can be described by a subgrain size δ and a sub-boundary misorientation θ, then[1]

$$\rho \propto \frac{\theta}{\delta} \qquad [6]$$

The relationship between the deformation features (δ and θ) of an individual grain and the average values ($\bar{\delta}$ and $\bar{\theta}$) of the polycrystalline aggregate can be expressed as

$$\frac{\theta}{\delta} = \left(\frac{M}{M_{av}}\right)^2 \frac{\bar{\theta}}{\bar{\delta}} \qquad [7]$$

where M_{av} is the average value of the Taylor factor. In addition, an empirical relationship between the average cell/sub-grain size $(\bar{\delta})$ and the deformation strain[22,23] is employed in the present work:

$$\bar{\delta} = 0.35 + 0.17/\varepsilon \qquad [8]$$

and

$$\bar{\delta}\,\bar{\theta}/\mathbf{b} = C \qquad [9]$$

where $\bar{\delta}$ is in microns, $\mathbf{b}$ is the Burgers vector, and C is a constant value between 60 and 80 rad. Equation [7] indicates that the stored energy is proportional to the square of the Taylor factor.

B. Nucleation and Growth

Based on the experimental data, nucleation is assumed to start from the original grain boundaries separating grains of different orientations. In a deformed grain with a specific orientation, the microstructure will have a variety of cell sizes and a distribution of misorientations. We assume that the microstructure can be described using two components:[24] an assembly of equiaxed subgrains and specific subgrains (effectively, subcritically sized recrystallization nuclei). The former can be characterized by a mean equivalent radius (R) and a mean misorientation (θ) and with boundaries of mean energy and mobility (γ and M_{sb}, respectively). The latter have a larger size ($R_n \sim 2.5R$) and different boundary characteristics ($\theta_n \geq 2.5\theta$, γ_n, M_n).

The effective nucleation-site density for grain-boundary nucleation is expressed by[25,26]

$$N_v = C_d S_v /\delta^2 \qquad [10]$$

where C_d is a calibration constant which determines the potential of the grain boundary as a nucleation site. The term S_v is the unit volume grain-boundary area, which is related to the original grain size (d), rolling strain (ε), and grain-shape tessellation in the space. For a tetrakaidecahedron, S_v varies with rolling strain in a manner described by[7]

$$S_v = \frac{1}{2d}(a + 3a\sqrt{1 + 2/a^2} + 3\sqrt{a^2 + 2/a^2} + \sqrt{2 + 2a^2}\Big/a \quad [11]$$

where $a = e^\varepsilon$ is the distortion along the rolling direction.

The driving pressure for growth of a particular grain is

$$P = -\frac{2\gamma_n}{R_n} + \frac{\alpha\gamma}{R} \quad [12]$$

where α is a geometrical constant and has a value of $\sim$1.5.[1]

The growth rate of a recrystallized grain is expressed as

$$\frac{dR_n}{dt} = M_n P = M_n\left(\frac{\alpha\gamma}{R} - \frac{2\gamma_n}{R_n}\right) \quad [13]$$

where $M_n(T)$ is the mobility of a high-angle boundary at the annealing temperature and which is given by

$$M_n(T) = M_0\exp(-Q/R_g T) \quad [14]$$

where M_0 is a pre-exponential factor, Q is the activation energy for boundary migration, R_g is the gas constant, and T is the annealing temperature.

The boundary energy is assumed to depend on the average misorientation angle only and is given by[1]

$$\gamma = \gamma_m\frac{\theta}{\theta_m}\left(1 - \ln\left(\frac{\theta}{\theta_m}\right)\right) \quad [15]$$

where γ_m and θ_m are the values of boundary energy and misorientation for high-angle boundaries, which are commonly taken as 0.324 J/m^2[1] and 15 deg, respectively. Combining Eqs. [9], [13], and [15], the relationship between the growth rate of a recrystallizing grain and the subgrain size of the assembly is approximately given by

$$V = \frac{dR_n}{dt} \simeq \frac{\alpha b C\gamma_m M_n}{\theta_m}\frac{1}{\delta^2} = \frac{K}{\delta^2} \quad [16]$$

with K being a temperature-dependent constant.

C. *Kinetics Approach*

The single-grain model described in Reference 7 is expanded along the lines described previously and is used to calculate the recrystallization kinetics in individual grains with a specific orientation. A nucleation event in an as-deformed grain is assumed to be site-saturated. A growing recrystallized grain is modeled as an expanding semisphere nucleated on grain boundaries. New grains grow independently of one another until hard impingement occurs.

As the position of the nuclei has a significant effect on the recrystallization kinetics,[7] the position of nuclei on the faces of the tetrakaidecahedron are determined randomly, assuming that there is an equal probability that each coordinate on the 14 faces (including grain edges and corners) may act as a nucleation site. Each simulation is, therefore, repeated a number of times (40) in the model calculation, and the average of the simulated kinetics is taken as the representative, *i.e.*, the time to obtain a given fraction of recrystallization (f) is given by the average over the number of simulations (j):

$$t_{av,i} = \sum t_{i,j}/j \quad [17]$$

where $t_{i,j}$ is the time at a given fraction in the jth simulation for a grain with a specific orientation labeled i.

Generally, a deformed polycrystal contains many grains of different orientations. Each grain has a different set of surrounding grains. In this attempt at modeling recrystallization kinetics in a polycrystal material, we assume that there is no correlation between the orientations of neighboring grains, and all the grains of one crystallographic orientation (within a certain small range) are represented by a single grain of the mean size. (The simulation results in the next section will show that this assumption is reasonable).

The overall kinetics of the polycrystalline aggregate can then be obtained by a weighted summation of the kinetics on the main textural components in the as-deformed state. The fractional recrystallization of the assembly is given by

$$f = \left(\sum\lambda_i f_i\right)\Big/\sum\lambda_i \quad [18]$$

where λ_i is the fraction of a main textural component.

IV. RESULTS

A. *Effect of the Grain Geometry and the Nucleation-Site Density on the Recrystallization Kinetics*

Before we present the simulation results, two new concepts need to be introduced, *i.e.*, the effective nucleation-site density and the numerical nucleation-site density. As long as C_d can be experimentally determined, the nucleation-site density (N_v) can be calculated using Eq. [10], which is called the effective nucleation-site density. In reality, a recrystallized grain at the original grain boundary may invade into two (or three) adjacent grains. However, in the single-grain kinetics model, the new grain is assumed to start from the original grain boundaries, and only the portion of the new grain inside the objective grain is taken into account when fractional recrystallization is calculated. As a consequence, only one-half of a physical nucleus is considered. Therefore, the numerical nucleation-site density, taken to be twice the effective nucleation-site density, is employed in calculating the nucleation sites in a single grain in the present model. In the model, the number of nuclei in a single grain calculated might be a noninteger. For such a case, the representative of the simulated recrystallization kinetics is treated as a weighted summation on the simulation kinetics obtained from simulations for the two nearest-integer nuclei per grain values.

In the single-grain kinetics model, the recrystallization fraction is proportional to $N(Vt/d)^3$, in which N is the number of

nuclei in an as-deformed grain of diameter d, t is real time, and $V = K/\delta^2$ is the growth rate. If the interface mobility is assumed to remain constant throughout the recrystallization process, to be independent of the applied deformation strain, and to remain constant for a certain number of N values, we can present the fraction of the recrystallized material as a function of the dimensionless reduced time (t^*), which is defined as

$$t^* = \frac{K}{\delta^2 d} t \qquad [19]$$

The real time can be calculated, provided K is known at a given annealing temperature.

Figure 3 shows the simulated recrystallization kinetics after a strain of 0.69, assuming that six nuclei are located randomly on the surface of a tetrakaidecahedron. Each curve represents one simulation. As can be seen, the simulated recrystallization kinetics differ from each other because of the difference in the nucleus positions. The difference in the kinetics reflects the characteristics of the nucleation nature. The six nuclei can either be present as clusters or can be far apart. When they form as a cluster, a slow recrystallization rate is obtained due to early impingement. Contrarily, when nuclei form far apart from each other, a faster rate will result. In order to obtain representative recrystallization kinetics for a fixed number of nuclei, we ran the simulations a number of times with different nucleation positions. We found that 40 simulations were adequate to yield a representative with a stable kinetics curve. In Figure 3, this average behavior is indicated by a square dotted curve. The representative curve shows a typical sigmoidal shape. The JMAK equation is only applied to the representative of simulation kinetics to obtain a least-squares best fit of the JMAK exponent, to determine the effects of underlying assumption and parameter values on n.

Figure 4 shows the simulated recrystallization kinetics for a tetrakaidecahedron of size $d = 100$ μm at different strains (0.41, 0.69, 1.10, 1.37, 1.61, and 2.3), with the number of nuclei per grain fixed at 6, and $\delta = 1$ μm. Because, in this subset of the simulations, we assume that the subgrain size does not change with the strain, then the kinetics after various degrees of rolling strain will only reflect the effect of

the grain geometry resulting from deformation on the recrystallization kinetics. As deformation increases, the aspect ratio of the grain increases, and the resulting n value decreases.

The preceding simulations are repeated to study the effect of the number of nuclei in an objective grain on the recrystallization kinetics. The resulting variations of n against strain for various numbers of nuclei are shown in Figure 5. It can be seen that the JMAK exponent depends on the number of nucleation sites. In a deformed tetrakaidecahedron, an increase in the number of nuclei gives a rise in n. However, in the case of the undeformed one, an opposite trend is found.

B. *Effect of the Strain on the Recrystallization Kinetics*

In reality, as strain increases, the subgrain size decreases, and S_v increases. Therefore, the nucleation-site density and the growth rate increase with strain. These factors favor the recrystallization kinetics. Figure 6 shows the simulated recrystallization kinetics in a tetrakaidecahedron with an initial size of 100 μm and average substructures after various

Fig. 4—The simulated recrystallization kinetics for the case of six nuclei located randomly on the surfaces of a tetrakaidecahedron at various strains. From leftmost to rightmost, $\varepsilon = 0.2$, 0.41, 0.69, 1.10, 1.37, 1.61, and 2.30.
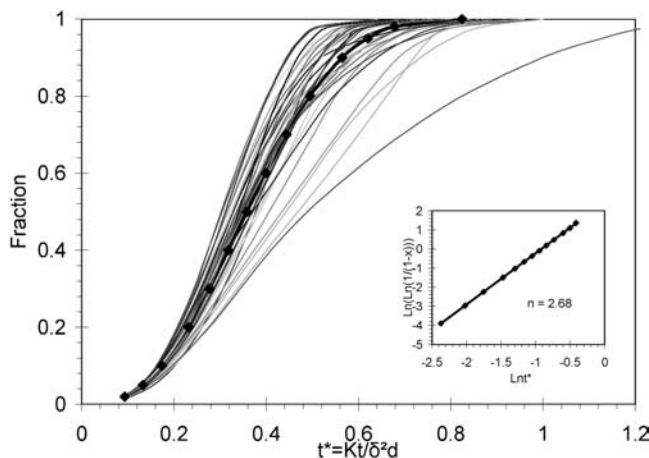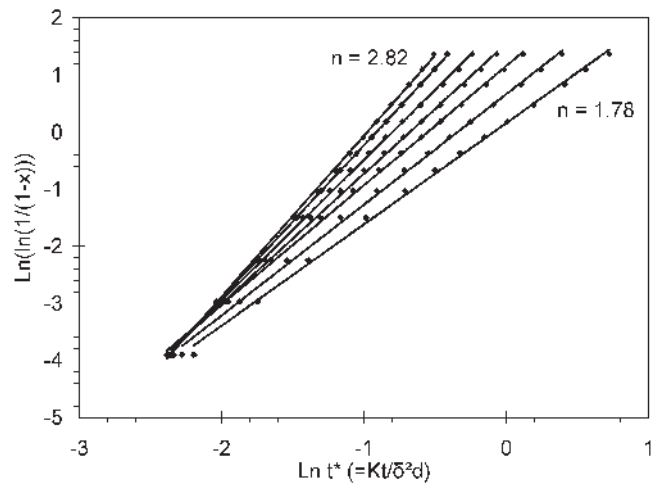

Fig. 3—Variation in recrystallization kinetics for the case of six nuclei located randomly on the surfaces of a tetrakaidecahedron at a strain of 0.69.
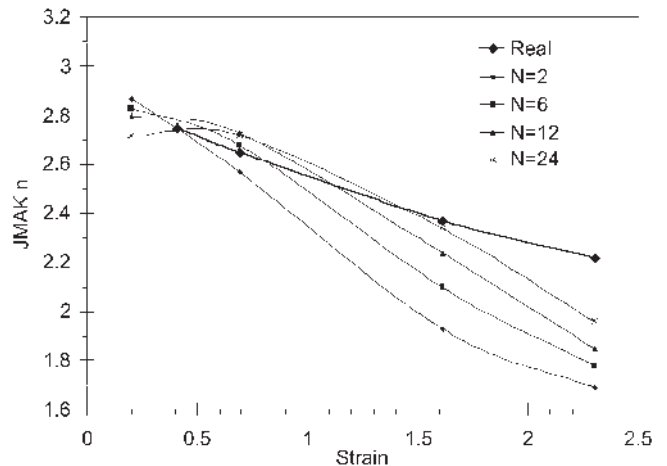

Fig. 5—Effect of the grain geometry resulting from deformation and the number of the nuclei on the JMAK exponent.

rolling strains. In these simulations, the subgrain size and the nucleation-site density at each strain are calculated according to Eqs. [8] and [10], respectively. The value of C_d is taken as 1.5×10^{-4} (which is calculated from the current experiment, and this value will be used in the following simulations). The fractional recrystallization is plotted against $(Kt/\delta_1^2 d_{100})$, with δ_1 being 1 μm. As can be seen, as the strain increases, the kinetics curves shift to shorter times, while the JMAK exponent decreases (which is shown in Figure 5 by the thick line with the caption "real"). The
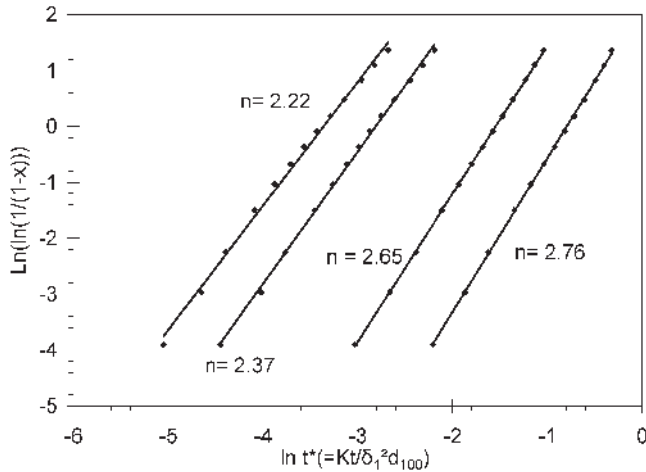

Fig. 6—The simulated recrystallization kinetics in a single grain after various strains. From leftmost to rightmost, $\varepsilon = 2.3$, 1.61, 0.69, and 0.41.

final variation of n with strain reflects the combined effect of the grain geometry and the nucleation sites. On the one hand, the increase in the number of nuclei will increase n. On the other hand, the grain-geometry change resulting from increasing strain leads to a lower value of n.

C. *Effect of the Initial Grain Size Prior to Deformation on the Recrystallization Kinetics*

Apparently, the initial grain size affects the nucleation-site density as it affects S_v, which decreases as the initial grain size increases. In addition, it can lead to a larger variation in stored energy resulting from variations in dislocation density after deformation. The second factor is most complicated, as it also depends on texture and orientation with respect to the deformation field, and will be considered later. In order to determine to which extent the initial grain size affects the recrystallization kinetics through S_v, we assume that the subgrain size does not change with strain and is fixed at 1 μm; then, the nucleation-site density at a given strain is only a function of the initial grain size. Figure 7 shows the simulated recrystallization kinetics, which is presented against $(Kt/\delta_1^2 d_{100})$, in the grains with three different initial diameters, i.e., 58, 100, and 200 mm, for four strain levels. As can be seen, the effect of the initial grain size on the recrystallization kinetics depends on the deformation strain applied. In an undeformed tetrakaidecahedron, a smaller grain does recrystallize faster than a coarser one. However, this effect decreases as the deformation strain increases. For example, at larger strains, the recrystallization kinetics in a coarser grain is faster than that in a finer
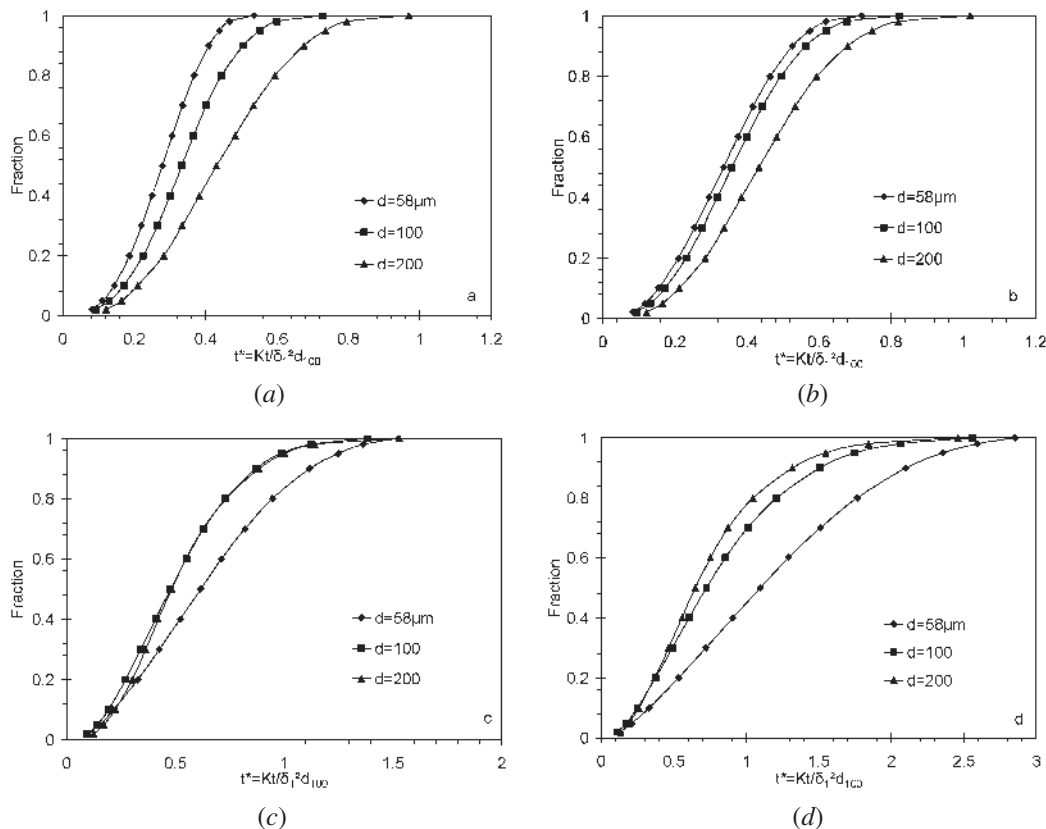

Fig. 7—The effect of the initial grain size on the recrystallization kinetics: (a) $\varepsilon = 0.2$, (b) $\varepsilon = 0.69$, (c) $\varepsilon = 1.61$, and (d) $\varepsilon = 2.30$.

grain. These results indicate that the increase in S_v resulting from deformation strain plays a dominant role in the increase of the nucleation density.

D. *Effect of the Orientation on the Recrystallization Kinetics*

Table I lists the Taylor factors of the main deformation textural components found in metals with an fcc crystal structure.[22,27] The Taylor factor of the Goss component is taken as an average of the values corresponding to the inclination of the shear band with respect to the rolling direction, these values being 30 and 35 deg, respectively. The related substructure parameters in grains with different orientations at a strain of 0.69 are calculated using Eqs. [7-9] and are listed in Table I. We assume that C_d has the same value for all grain boundaries and equals 1.5×10^{-4} when calculating the nucleation-site density in grains with different textural components. Figure 8 shows the simulated recrystallization kinetics in grains with different orientations, but with a fixed initial grain size of 100 μm at a strain of 0.69. As can be seen, a grain with a larger Taylor factor recrystallizes earlier and at a higher rate.

V. APPLICATION OF THE MODEL TO THE EXPERIMENT DATA

As indicated previously, the overall recrystallization kinetics should include the effect of the grain geometry, the nucleation-site density, the starting grain size, and the strain variation from grain to grain as a consequence of the grain orientation. The grain-size distribution in annealed materials is approximately log-normal, where the maximum grain size is typically 2.5 to 3 times the mean size. To determine the overall recrystallization kinetics of the grains with different sizes, we can apply the method specified in Reference 7. However, from the proceeding simulation results, we have realized that the grain orientation has a much stronger effect on the recrystallization kinetics than the initial grain size. Hence, for the sake of

simplicity, we assume in the overall recrystallization kinetics that all the grains with a particular crystallographic orientation can be represented by a single grain of mean size.

Now, the single-grain model can be applied to predict the recrystallization kinetics if the input parameters of the deformation strain (ε), initial grain size (d), calibration constant (C_d), mobility at a given annealing temperature (M_n), and volume fraction of the main texture components in the as-deformed state are determined.

In the current experiment on AA1050, the initial grain size prior to deformation, as well as the fully recrystallized grain size after deformation to a strain of 0.69 and annealing at 340 °C, are taken to be 100 and 69 μm, respectively. From these values, the number of the effective nuclei in a single grain of mean size is estimated to be 3, leading to a calibration constant of 1.5×10^{-4}. The corresponding nucleation-site density and subgrain size in a grain with a given orientation are determined according to Section IV–D. Since M_n could not be determined from the present experiment, we leave it as a free parameter in the model. The simulated recrystallization kinetics in grains with different orientations is shown in Figure 8.

The overall recrystallization kinetics can be obtained now using Eq. [18] and considering the frequency of the texture components in the deformed state listed in Table I. The resulting curve is shown in Figure 8 by the square dotted line. The Avrami plots of the experimental data and the simulation are shown in Figure 9. The JMAK exponents measured and simulated are 1.99 and 1.94, respectively. Obviously, the present model could yield a much more practical prediction of the JMAK n exponent by taking into account the deformation inhomogenity from grain to grain due to variations of the Taylor factor.

VI. DISCUSSION

The simulation results from the present model show that the JMAK exponent of a apparent recrystallization-kinetics curve depends on the grain geometry, nucleation-site density, initial grain size prior to deformation, and main textural components
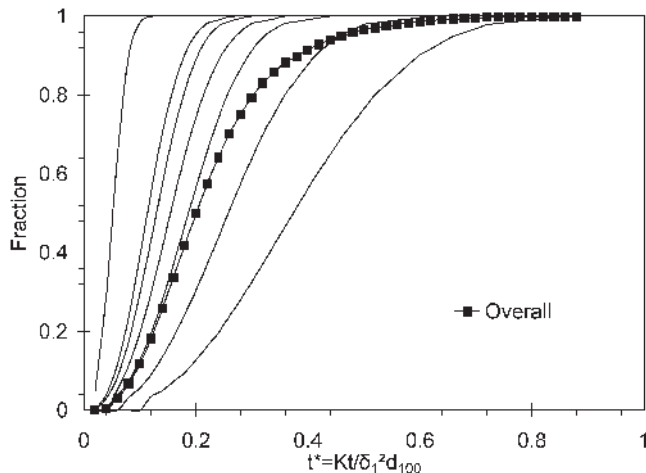
Fig. 8—The simulated recrystallization kinetics in grains with different orientations and overall recrystallization kinetics in AA1050. Thin solid line: from leftmost to rightmost, RG, copper, S, brass, random, goss, and cube. Square dotted line: the overall recrystallization kinetics.
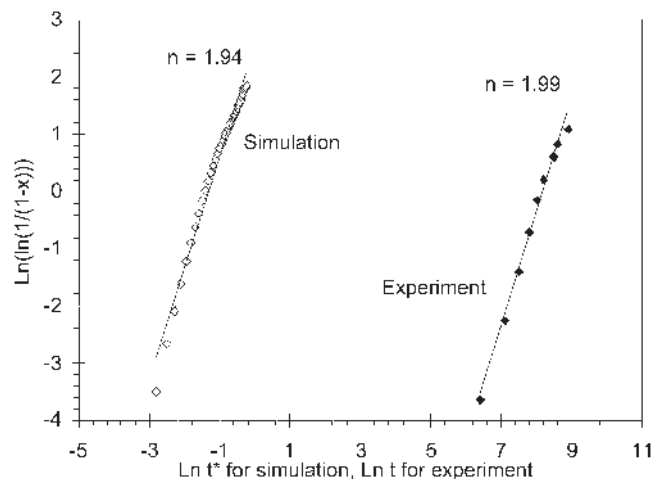
Fig. 9—The comparison of the experiment with the prediction from the single grain model by considering orientation-dependent kinetics.

after deformation. This result, which is one of the important features that the present model reveals, implies that the recrystallization space (the space that the recrystallizing grains grow into) is of importance in deciding the recrystallization kinetics. In real materials, recrystallization space is effectively defined by both the initial grain size and the deformation geometry. The change of the grain geometry due to deformation leads to a change in the impingement space of the recrystallized grains. An increase in the number of nuclei will also cause a change in the impingement space.

Another salient feature that the present refined model shows is that the effect of the texture components in the as-deformed state on the recrystallization kinetics is significant. This point will be elaborated further by simulations. Figure 10 shows the simulated orientation-dependent recrystallization kinetics at two strain levels, 0.69 and 1.61, respectively. We use the two starting structures with different fractions of texture components, as listed in Table II. The
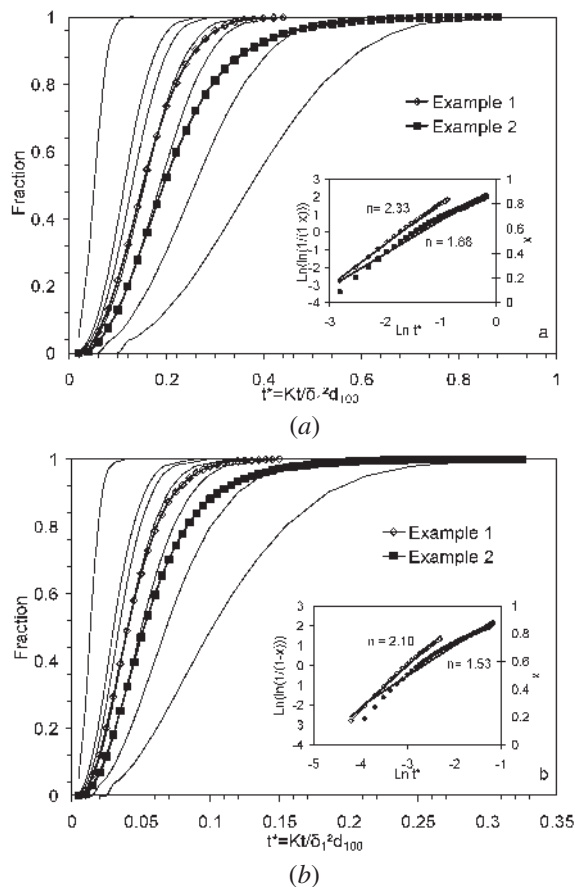

(a)

(b)

Fig. 10—The simulated recrystallization kinetics in grains with different orientations and overall recrystallization kinetics of two examples. Thin solid line: from leftmost to rightmost, RG, copper, S, brass, random, Goss, and cube. (a) $\varepsilon = 0.69$ and (b) $\varepsilon = 1.61$.

overall kinetics curves of two examples are indicated in Figure 10 as well. In the same figure in the smaller box, the Avrami plots for these two examples are plotted. It can be seen that shape and the slope of the JMAK plot are related to the mixture of the texture components. When there are Goss and cube texture components present in the as-deformed state, the JMAK plot shows a nonlinear behavior, i.e., two-stage n, which has been frequently reported in the literature.

Many factors that control recrystallization are not specifically treated in the JMAK model, but are casually lumped into the constants in Eq. [1]. Two important factors that are included in this category are the initial grain size prior to deformation and the amount of deformation. These points can be clarified with the help of the present model.

Theoretical studies in the literature suggested that the finer-grained material recrystallizes after a shorter incubation time and within a shorter relative time period than the coarser-grained material, although the actual experiments yielded controversial results.[28,29] Generally, since recrystallization nucleates primarily along prior grain boundaries, the rate of nucleation is directly proportional to S_v, which increases as the grain size decreases. Therefore, after similar amounts of deformation and for similar growth rates, the rate of recrystallization should increase as the prior grain size decreases. However, if it is assumed that the substructure in a fine grain and a coarse one is equal (this is true for aluminum alloys at strains larger than 0.5[30]) and that the fraction of the texture components is the same in both cases, the present model shows that it depends on the strain level whether small grains recrystallize faster or slower than large grains. At lower strains, small grains recrystallize faster. However, at larger strains, the recrystallization rate in coarser grains becomes higher. This is attributed to the change in the impingement space due to the deformation geometry and the relatively large number of nucleation sites in the coarser grains as strain increases. This prediction is in excellent agreement with an experimental study by Sellars's group.[31] It should be pointed out explicitly that the mechanism of intragranular nucleation in larger strains need not be involved to explain this result, as, in the current simulations, nucleation always occurs at the grain boundaries.

Finally, the initial grain size and the amount of strain are both known to have a large effect on the texture components in the as-deformed state. As can be seen from Figure 11, which shows the textural-component evolution with cold-rolling strain in a commercial aluminum alloy,[32] the rolling-texture components intensify while the fraction of the soft components (Goss and cube) decreases with increasing strain. The variation of the textural concentration with strain in the fine-grained material is different from that in the coarse-grained one. Therefore, the initial grain size and the degree of deformation can affect the recrystallization kinetics through their effect on the texture components. The model correctly predicts this changeover in relative behavior.

Table II. The Frequency of Textural Components in the As-Deformed State for Two Assumed Structures

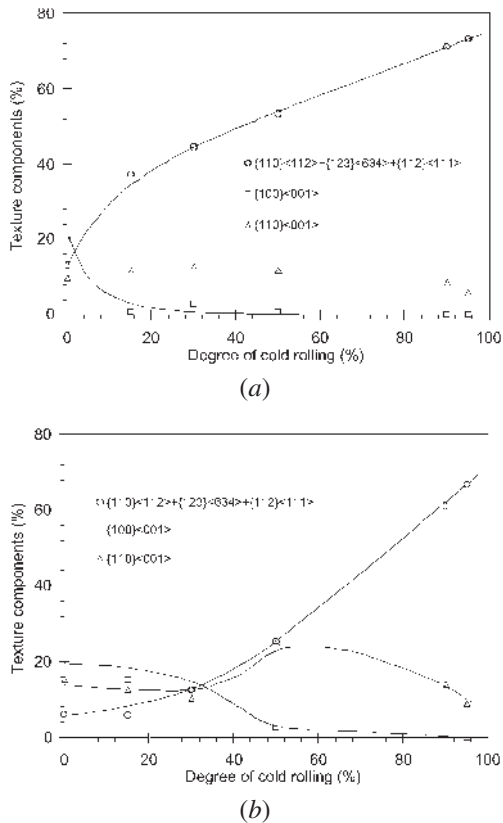| Texture Components	Copper	S	Brass	Goss	Cube	Random
Example 1	16	20	23	0	0	41
Example 2	3	8	12	22	8	47

Fig. 11—The volume fractions of the texture components in the cold-rolled AA1050 as a function of the degree of deformation: (*a*) fine initial grain size (50 μm) and (*b*) coarse initial grain size (350 μm).[32]

VII. CONCLUSIONS

The following conclusions are obtained from the refined recrystallization model, which incorporates both the deformed microstructure and the textural components.

1. The kinetics model based on the single approach provides new insight to gain a better understanding of annealing phenomena in deformed polycrystals, particularly the effect of nonrandom nucleation sites and the geometry by which recrystallized grains fill space, on recrystallization kinetics.
2. The simulation shows that the JMAK exponent depends on the grain geometry, nucleation-site density, initial grain size prior to deformation, and main textural components after deformation. The effect of grain size on the recrystallization kinetics depends on the amount of prior strain applied.
3. After introducing the deformation inhomogeneity from grain due to differences in the Taylor factor, the single-grain approach could predict correctly the JMAK exponent.

REFERENCES

1. F.J. Humphreys and M. Haltherly: *Recrystallization and Related Annealing Phenomena*, Pergamon, London, 1996.
2. R.A. Vandermeer and P. Gordon: *Recovery and Recrystallization of Metals*, Interscience, New York, NY, 1962.
3. R.A. Vandermeer and B.B. Rath: *Metall. Trans. A*, 1990, vol. 21A, pp. 1143-49.
4. R.A. Vandermeer and B.B. Rath: *Metall. Trans. A*, 1989, vol. 20A, pp. 391-401.
5. E.C.W. Perryman: *Trans. AIME, J. Met.*, 1955, vol. 203, pp. 1053-61.
6. R.A. Vandermeer and B.B. Rath: in *Simulation and Theory of Evolving Microstructures*, M.P. Anderson and A.D. Rollett, eds., TMS, Warrendale, PA, 1990, pp. 119-26.
7. S.P. Chen, I. Todd, and S. van der Zwaag: *Metall. Mater. Trans. A*, 2002, vol. 33A, pp. 529-37.
8. L. Delannay, O.V. Mishin, D.J. Jensen, and P. van Houtte: *Acta Mater.*, 2001, vol. 49, pp. 2441-51.
9. V. Randle, H. Hansen, and D.J. Jensen: *Phil. Mag. A*, 1996, vol. 73, pp. 265-82.
10. T. Furu, K. Marthinsen, and E. Nes: *Mater. Sci. Technol.*, 1990, vol. 6, pp. 1093-102.
11. A.D. Rollett, D.J. Srolovitz, R.D. Doherty, and M.P. Anderson: *Acta Metall.*, 1989, vol. 37, pp. 627-39.
12. E. Nes and J.K. Solberg: *Mater. Sci. Technol.*, 1986, vol. 2, pp. 19-23.
13. E.C.W. Perryman: *Trans. AIME, J. Met.*, 1955, vol. 203, pp. 369-78.
14. I.L. Dillamore and H. Katoh: *Met. Sci.*, 1974, vol. 8, pp. 73-83.
15. W.B. Hutchinson: *Met. Sci.*, 1974, vol. 8, pp. 185-96.
16. D.P. Field and H. Weiland: *Mater. Sci. Forum*, 1994, vol. 157–162, pp. 1181-88.
17. X.Y. Wen and W.B. Lee: in *Sheet Metal Forming Technology*, M.Y. Demeri, eds., TMS, Warrendale, PA, 1999, pp. 233-43.
18. E.M. Lauridsen, D.J. Jensen, H.F. Poulsen, and U. Lienert: *Scripta Mater.*, 2000, vol. 43, pp. 561-6.
19. R.D. Doherty, D.A. Hughes, F.J. Humphreys, J.J. Jonas, D.J. Jensen, M.E. Kassner, W.E. King, H.J. McQueen, and A.D. Rollett: *Mater. Sci. Eng. A*, 1997, vol. 238, pp. 219-74.
20. S.P. Chen, D. Hanlon, S. van der Zwaag, Y.T. Pei, and J.T.M. de Hosson: *J. Mater. Sci.*, 2002, vol. 37, pp. 989-95.
21. J. Gil Sevillano, P. van Houtte, and E. Aernoudt: *Scripta Metall.*, 1976, vol. 10, pp. 775-78.
22. J. Gil Sevillano, P. van Houtte, and E.A.D. Aernoudt: *Progress. Mater. Sci.*, 1980, vol. 25, pp. 69-412.
23. N. Hansen and D.A. Hughes: *Phys. Status Solidi (b)*, 1995, vol. 149, pp. 155-72.
24. F.J. Humphreys: *Acta Mater.*, 1997, vol. 45, pp. 4231-40.
25. C.M. Sellars: in *Thermomechanical Processing in Theory, Modeling & Practice [TMP]*², B. Hutchinson *et al.*, eds., Swedish Society for Metals Technology, ASM Stockholm, Sweden, 1996, pp. 35-51.
26. H.E. Vatne, T. Furu, R. Orsund, and E. Nes: *Acta Mater.*, 1996, vol. 44, pp. 4463-73.
27. H.J. Bunge: *Texture Analysis in Materials Science*, Butterworth and Co., London, 1982.
28. J.C. Blade and P.L. Morris: *Proc. 4th Int. Conf. on Textures*, Cambridge, Cambridge University Press, United Kingdom, 1975, pp. 171-78.
29. L. Ryde, W.B. Hutchinson, and S. Jonsson: in *Recrystallization '90*, T. Chandra, eds., TMS, Warrendale, PA, 1990, pp. 313-18.
30. P. Cotterill and P.R. Mould: *Recrystallization and Grain Growth in Metals*, Surrey University Press, London, 1976.
31. P.L. Orsetti Rossi and C.M. Sellars: *Aluminium Alloys, Their Physical and Mechanical Properties*, Proc. 6th Int. Conf. on Aluminium Alloys, ICAA-6, T. Sato, S. Kumai, T. Kobayashi, and Y. Murakami, eds., The Japan Institute of Light Metals, Toyohashi, Japan, 1998, vol. 2, pp. 1227-32.
32. N. Hansen and D.J. Jensen: *Metall. Trans. A*, 1986, vol. 17A, pp. 253-59.